

## Optical excitations in poly(2,5-thienylene vinylene)

A. J. Brassett, N. F. Colaneri, D. D. C. Bradley,  
R. A. Lawrence, and R. H. Friend

*Cavendish Laboratory, University of Cambridge, Madingley Road, Cambridge CB3 0HE, United Kingdom*

H. Murata, S. Tokito, T. Tsutsui, and S. Saito

*Department of Materials Science and Technology, Interdisciplinary Graduate School of Engineering Sciences,  
Kyushu University, Kasuga-shi, Fukuoka 816, Japan*

(Received 16 October 1989)

We present the results of spectroscopic studies of the electronic structure of the conjugated polymer poly(2,5-thienylene vinylene). Photoexcitation above the band gap at 1.8 eV gives rise to two transient absorption peaks at 0.44 and 1.0 eV that are associated with bipolarons that live for times of order a few milliseconds at 80 K. Photoluminescence, comparable in intensity to the Raman scattering, is found at energies above the band edge, and we assign this to a hot recombination process. We also report the Raman spectrum, and make a preliminary assignment of the main vibrational modes. Three of the four main peaks disperse as the excitation wavelength is varied. We discuss these results and compare them with those previously reported for a related polymer, poly(*p*-phenylene vinylene).

### I. INTRODUCTION

There is considerable interest in the potential application of conjugated polymers in electro-optical and nonlinear optical devices.<sup>1</sup> The poly(arylene vinylene) polymers of general formula  $[-A-\text{CH}=\text{CH}-]_n$  (where *A* is an aromatic or heteroaromatic moiety such as phenylene, naphthalene, or thienylene) are one particular class of conjugated polymer currently under extensive investigation.<sup>2,3</sup> In addition to satisfying the apparently general requirement for a significant third-order optical susceptibility in polymers, namely the possession of a delocalized, and hence readily polarizable electronic structure, the poly(arylene vinylene) polymers have the distinct advantage of being prepared via a synthetic route that allows considerable flexibility for sample preparation. This so-called "precursor route" involves the synthesis of a solution processible, nonconjugated precursor polymer that can be readily converted to the conjugated material by an appropriate thermal treatment. Fabrication into the desired sample form (e.g., high-optical-quality, fully dense, homogeneous thin films) is carried out prior to the thermal conversion step, thus circumventing the difficulties associated with the rigidity of the conjugated structure. Moreover, since chemical modification of the arylene group or its replacement by a heteroarylene group results in a systematic variation in electronic structure, the poly(arylene vinylene)s are also of more fundamental interest for gaining a detailed un-

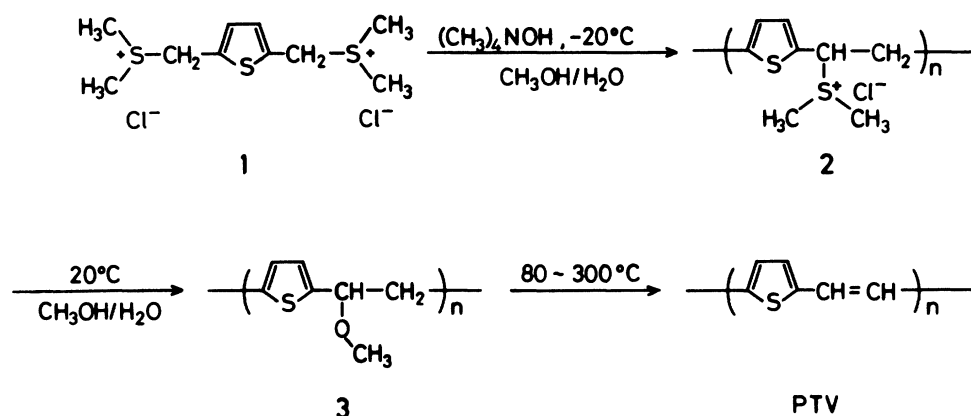
derstanding of the electronic properties of conjugated polymers in general.

To date, the most extensively studied of the poly(arylene vinylene)s has been poly(*p*-phenylene vinylene) (PPV) (Refs. 4 and 5), which shows promise for nonlinear optical applications<sup>2</sup> because of its high optical nonlinearity, subpicosecond response time, and excellent environmental, mechanical, and thermal stability. In this paper we use photoinduced absorption and photoluminescence to study the effect of the replacement of the phenylene by a thienylene moiety upon the excited states of the polymer. This polymer, poly(2,5-thienylene vinylene) (PTV) has been found<sup>6</sup> to have a band gap 25% lower than that of PPV.<sup>4</sup> We also find that its photoluminescent yield is nearly 4 orders of magnitude lower. In addition, the level structure of the metastable charged states generated by photoexcitation suggests that the  $\pi$ -electron system of PTV behaves more like that of polyacetylene than any other conjugated polymer that has thus far been investigated. Measurements of third-harmonic generation in PTV have been reported in an earlier paper.<sup>3</sup>

### II. SAMPLE PREPARATION AND EXPERIMENTAL DETAILS

The samples of PTV used in this study were synthesized via a modified sulphonium polyelectrolyte pre-

cursor route as shown below:



The methoxy pendant precursor polymer (3) was prepared in two steps. First, base-induced polymerization of the 2,5-thienylene-bis(methylene dimethylsulfonium chloride) monomer (1) was carried out in a water-methanol mixture at  $-20^\circ\text{C}$  by adding a methanol solution of tetramethylammonium hydroxide. The reaction was quenched by the addition of hydrochloric acid. This yielded a pale yellow solution of the sulfonium polyelectrolyte polymer (2), which was subsequently warmed up to room temperature so as to facilitate the sulfonium displacement reaction with methanol. The resulting product (3) was isolated as a precipitate, then filtered and vacuum dried before being purified by reprecipitation from chloroform into diethylether. Further details of the synthesis and characterization of (3) are given elsewhere.<sup>6</sup> As shown in the scheme above, conversion of the precursor polymer to conjugated PTV requires the elimination of one methanol group per monomer unit. In order to drive the reaction to completion, it was found necessary to utilize an acid catalyst in addition to the more usual heat treatment (in-vacuo or under inert-gas atmosphere) that suffices for conversion of the sulfonium polyelectrolyte precursor of PPV.<sup>4</sup> Full conversion was typically achieved by heating at temperatures between 100 and  $200^\circ\text{C}$  under flowing  $\text{N}_2$  containing dry-gaseous  $\text{HCl}$ . Conversion was confirmed by checking for the absence of the characteristic vibrations of the saturated precursor groups in the infrared spectrum, and the absence of a signal from  $sp^3$ -hybridized carbons in the high-resolution solid-state  $^{13}\text{C}$  NMR.<sup>6</sup>

For optical measurements thin films of the PTV precursor were spin coated onto sapphire substrates from tetrahydrofuran (THF) solution. After thermal conversion to PTV, the samples had a typical optical density of order 1.5–2.5 at the peak in their absorption spectra. Film thicknesses, determined from their reflectivity by a multiple-beam interference technique, were between 80 and 140 nm. Hence, the peak absorption coefficient is of order  $2 \times 10^5 \text{ cm}^{-1}$ .

Optical measurements were performed in an Oxford Instruments CF-204 optical-access helium cryostat, allowing temperature control between 10 K and room temperature. Thermal contact to the samples was provided by a helium exchange gas within the sample space. Absorption and induced-absorption measurements were per-

formed in the visible- and near-infrared spectral regions (0.4–4 eV) using a tungsten halogen source, dispersed with a grating monochromator and measured with a photomultiplier tube, silicon photodiode, or cooled indium antimonide detector.

Photoinduced absorption was measured by probing the absorption of light from the tungsten halogen lamp during laser photoexcitation. The green, blue, and ultraviolet lines from a Coherent, Inc. Innova-100 argon-ion laser were used to photoexcite the sample. By mechanically chopping the laser light and using phase-sensitive detection methods, the transient optical response of PTV in the frequency range  $60 \leq \omega \leq 2.5 \times 10^4 \text{ rad/s}$  was accessible.

Luminescence and Raman spectra were recorded at room temperature in a  $90^\circ$  scattering geometry, using a modified Coderg PH1 double-grating monochromator and a Hamamatsu R943-02 photomultiplier tube. The excitation beam was provided either by the argon-ion laser or by using the argon-ion laser to pump 4-(dicyanomethylene-*z*-methyl-6-(*p*-dimethyl-amino-styryl)-4*H*-pyran (DCM) in a Coherent, Inc. 590 dye laser. This provided a range of excitation wavelengths between 457.9 and 656.0 nm.

### III. RESULTS

The PTV films obtained as described above are fully dense (density of  $1.33 \text{ g/cm}^3$  determined by flotation) but show a degree of crystallinity lower than that of PPV.<sup>6</sup> Their intrinsic conductivity is less than  $10^{-13} \text{ S/cm}$  although if measured in air, oxygen doping leads to a typical value of  $10^{-7} \text{ S/cm}$ . Doping with iodine yields conductivities as high as  $200 \text{ S/cm}$ , and the doped samples are found to be stable in air.<sup>6</sup>

#### A. Optical absorption

Optical-absorption spectra are shown in Fig. 1. At room temperature, the onset of the  $\pi$ - $\pi^*$  transition in PTV occurs just below 1.8 eV, and the absorption edge shifts to lower energies at lower temperatures, by about 0.03 eV lower at 15 K. In addition, the phonon features in the absorption edge, spaced by about 0.18 eV, become more pronounced as the temperature is decreased. These

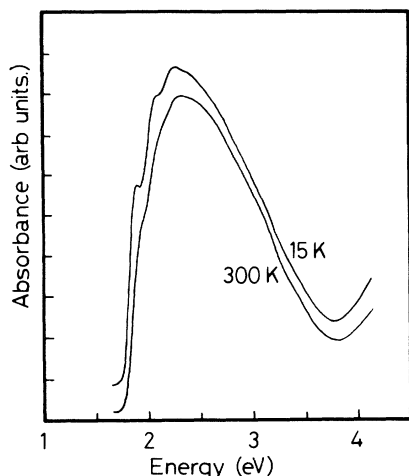


FIG. 1. Optical-absorption spectra for a PTV thin film recorded at both 300 and 15 K. The spectra are displaced vertically for clarity.

features are more clearly visible in a measurement of the thermal modulation of the absorption edge. The fractional change in transmission upon heating the sample from 80 to 100 K is plotted in Fig. 2. This difference spectrum shows three sharp derivative features with local maxima at 1.82, 2.03, and 2.21 eV, corresponding to the phonon peaks in the absorption spectrum.

### B. Resonance Raman spectroscopy

The Raman spectrum of PTV for excitation at 457.9 and 656 nm is shown in Fig. 3. Four main bands are clearly seen, with peaks at 1042, 1282, 1405, and 1580  $\text{cm}^{-1}$  when excited at 656 nm. Additional weak features may also be present, but these are not well resolved due, in part, to a luminescence background that appears as a constant intensity offset of comparable strength to the Raman signal. The detailed assignment of the observed

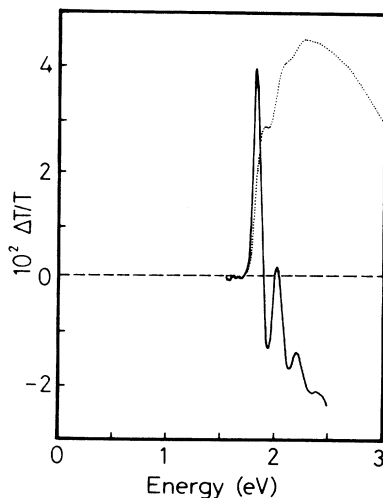


FIG. 2. Thermal modulation spectrum for PTV obtained as the fractional difference in optical transmission between the absorption spectra recorded at 80 and 100 K,  $-\Delta T/T \equiv [T(80 \text{ K}) - T(100 \text{ K})]/[T(80 \text{ K})]$ . For comparison we also show the absorption spectrum at 80 K.

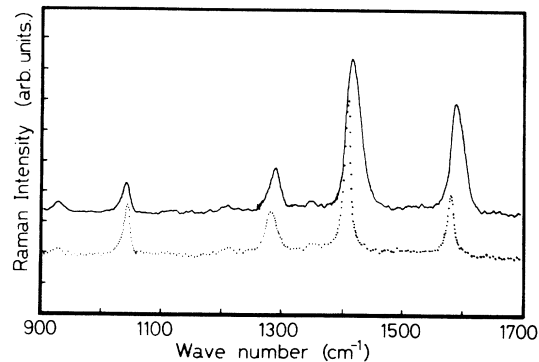


FIG. 3. Resonance Raman spectrum of PTV recorded with excitation at (a) 656 nm (1.89 eV) (data points) and (b) 457.9 nm (2.71 eV) (solid line).

Raman peaks to specific vibrational modes of the PTV chain has not yet been made. However, through comparison with the spectra for poly(thiophene) (Ref. 7) and PPV (Ref. 8) we can make a preliminary assignment of the peaks at 1042 and 1405  $\text{cm}^{-1}$  to vibrations predominantly associated with the thienylene moiety and those at 1282 and 1580  $\text{cm}^{-1}$  to vibrations more closely linked with the vinylene moiety. The peak at 1042  $\text{cm}^{-1}$  is most likely a thienylene CH in-plane bending mode analogous to that seen at 1045  $\text{cm}^{-1}$  in poly(thiophene).<sup>7</sup> That at 1405  $\text{cm}^{-1}$  is expected to be a stretching mode largely involving motion of the thienylene  $\alpha$ -C. Its low frequency, in comparison to the equivalent 1460- $\text{cm}^{-1}$  peak in poly(thiophene),<sup>7</sup> is consistent with a softening of the mode through an increased  $\pi$ -electron delocalization along the chain due to introduction of the vinylene moiety. We consider the 1580- $\text{cm}^{-1}$  peak to be another stretching mode but in this case largely of the vinylene double bond. The frequency shift from 1628  $\text{cm}^{-1}$  for the equivalent model in PPV (Ref. 8) is as expected for a more uniform  $\pi$ -electron bond order along the polymer chain. We note that the frequency for the double-bond stretch mode in *cis*-polyacetylene is at 1541  $\text{cm}^{-1}$ .<sup>9</sup> Finally, the peak at 1282  $\text{cm}^{-1}$  is interpreted as arising from a vibration that has a strong CH in-plane bending character analogous to that seen at 1330  $\text{cm}^{-1}$  in PPV (Ref. 8) and to the weak peak at 1290  $\text{cm}^{-1}$  in *trans*-polyacetylene.<sup>9</sup>

Of the four peaks, that at 1042  $\text{cm}^{-1}$  is the only one that does not shift in frequency as the excitation wavelength is scanned across the absorption band of Fig. 1. We find that the three peaks at 1282, 1405, and 1580  $\text{cm}^{-1}$  gradually shift up in energy until, for excitation at 457.9 nm as shown in Fig. 3, they appear at 1289, 1416, and 1588  $\text{cm}^{-1}$ . In addition, the two higher-energy peaks both broaden significantly and the highest-energy peak increases strongly in relative intensity. Similar dispersion effects are well known for the Raman spectra of *trans*-polyacetylene<sup>9,10</sup> and to a lesser extent poly(thiophene),<sup>11</sup> and are interpreted as being due to a resonance selection of polymer chains with differing degrees of bond order. The modes that disperse are those for which the electron-phonon coupling strength, and hence the vibrational force constants, depend upon the effective conjugation length of a polymer chain segment.<sup>10</sup> The dispersion

then arises because these chain segments also have different optical band gaps and thus, as the excitation wavelength is varied, the Raman spectrum is successively dominated by resonantly enhanced contributions at different vibrational frequencies.

For comparison, we note that in PPV the frequencies of the Raman active modes are essentially independent of excitation energy.<sup>8</sup> This does not, however, necessarily mean that within a typical PPV sample there is a mono-disperse conjugation length. We consider, rather, that the vibrational force constants in PPV are largely insensitive to the polymer chain length. We note that the Raman frequencies for the PPV oligomer *trans,trans*-1,4-distyrylbenzene are within a wave number or two of those of the corresponding modes for the polymer.<sup>12</sup> We can understand this behavior in terms of the constraint that the stabilization energy of an aromatic configuration for the phenylene ring puts upon the overall chain geometry.

A more detailed analysis of the resonance Raman dispersion in PTV should allow us to characterize the disorder present within our samples.<sup>13</sup> The enhanced sensitivity of this technique relative to x-ray diffraction or infrared- and ultraviolet-visible spectroscopy derives from its resonance selection of the disordered polymer sequences. Thus, the sharp band edge and resolved phonon structure in Fig. 1, indicative of a rather narrow conjugation length distribution, are not inconsistent with the dispersion of the resonance Raman scattering.

### C. Photoluminescence

In contrast to the photoluminescence (PL) in PPV which is strong, with a quantum yield of several percent,<sup>5,14</sup> in PTV we find that it is very weak, and observable only as a broad background to the Raman signal. Figure 4 shows this photoluminescence following excitation of the sample with the 457.9-nm line of the argon-ion laser. The figure also shows that the slight oxidative doping of the sample due to handling in air leads to a quenching of the luminescence, a process that can be reversed by heating to 150°C under high vacuum for several hours. The spectral profile of the photoluminescence band depends in detail on the wavelength of excitation, but all of the emission always appears above the band edge at 1.8 eV. Because the photoluminescence intensity is of the same order as that of the Raman signal, we estimate the quantum yield to be  $\sim 10^{-5}$ . This is similar to the value for *cis*-polyacetylene<sup>15</sup> but is nearly 4 orders of magnitude smaller than the quantum yield of  $\sim 0.08$  that is estimated for PPV.

### D. Photoinduced absorption

Experiments on a number of conjugated polymers have established that some of the electron-hole pairs generated by laser photoexcitation above the band edge separate effectively, escaping prompt geminate recombination, and resulting in the formation of charged excitations that can be stable on timescales of order milliseconds or longer. The self-consistent distortion of the lattice associated with these photogenerated charged states leads to a significant shift of oscillator strength from the interband

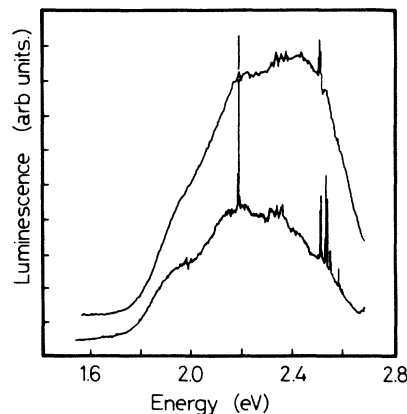


FIG. 4. Photoluminescence from PTV following excitation at 457.9 nm. The upper spectrum (displaced for clarity) was recorded after heating the film at 150°C under a vacuum of  $10^{-4}$  mbar for 12 h.

transition to new discrete levels deep in the gap. We show the photoinduced absorption (PA) spectrum of PTV at 80 K in Fig. 5. To obtain the data below 2.3 eV the sample was photoexcited with about 200 mW/cm<sup>2</sup> of the 488 nm (2.54 eV) line and for the data above 2.3 eV excitation was with the multiline uv output of the argon-ion laser, though data below 2.3 eV were similar for both excitation energies. Two absorption features [ $\sim 0.7$  eV full width at half maximum (FWHM)] appear below the band edge, peaking near 1 and 0.44 eV. On the basis<sup>16</sup> of the number of peaks and their position relative to the band edges, we assign them to subgap transitions associated with bipolarons, the long-lived charged species that typically result from photoexcitation of a nondegenerate-ground-state polymer.<sup>17</sup> Their identification as resulting from charged excitations is consistent with the previously reported observation of photoinduced

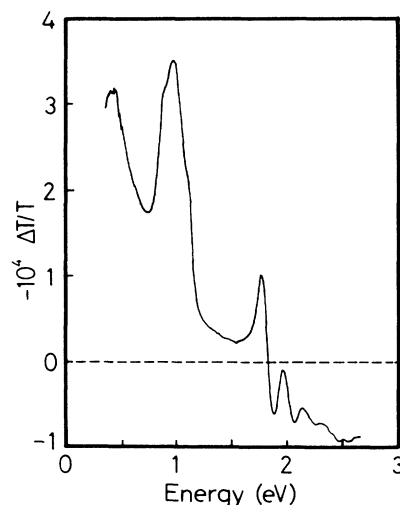


FIG. 5. The photoinduced absorption spectrum of PTV recorded at 80 K following chopped cw excitation at 488 nm. The data above 2.3 eV were recorded with excitation by the multiline uv output of the Ar<sup>+</sup> laser.

infrared-active vibrational modes in PTV (Ref. 18). The energy separation of the two subgap features, only 0.56 eV, is much smaller than that which has been measured in other nondegenerate-ground-state conjugated polymers such as PPV,<sup>5,14</sup> poly(thiophene),<sup>19</sup> poly(3-hexyl thiophene),<sup>20</sup> and polydiacetylene<sup>21</sup> and as discussed below suggests that the degree of confinement in this material is small.

Associated with the induced absorption below the band edge, we expect to find photoinduced bleaching (PB) at and above the band edge, to satisfy the sum rule

$$\int_0^{\infty} \delta\alpha(\omega) d\omega = 0, \quad (1)$$

where  $\delta\alpha$  is the change in absorption coefficient at frequency  $\omega$ . The photoinduced absorption spectrum of PTV shows a general shift to induced bleaching above the band edge, but it is clear that the bleaching must extend far into the uv to satisfy the sum rule. Superimposed on this, we observe three regularly spaced derivative features with maxima at energies 1.78, 1.97, and 2.15 eV. These features can be attributed to electromodulation of the band edge due to local fields associated with the presence of charged photoexcitations. This is well established in the case of polyacetylene prepared by the Shirakawa route,<sup>22,23</sup> for which the electroabsorption signal was found to reproduce the photoinduced band-edge features, with both spectra varying with probe photon frequency as  $\partial^2\alpha/\partial\omega^2$ . The thermal modulation (TM) spectrum, however, varies as  $-\partial\alpha/\partial\omega$ ,<sup>22</sup> and we note that, as expected, the TM signal shown in Fig. 2 is of opposite sign to the PA at the band edge and blue shifted (by 0.05 eV). As discussed below, measurements of the temperature, laser intensity, and chop-frequency dependence of the photoinduced subgap transitions and band-edge features of Fig. 5 confirm that they have a common origin.

The dependence of the strength of the transitions at 0.44 and 1 eV on laser intensity is sublinear. The data in Fig. 6 show the magnitude of the photoinduced absorption signal at 1 eV as a function of laser intensity, again measured at 80 K. For this measurement, the sample was photoexcited with the 488-nm (2.54-eV) line of the argon-ion laser. The solid line in the figure is a fit of the data to a function of the form  $I^{1/2}$ , the square root of the laser intensity, and is consistent with a bimolecular mechanism of decay. The band-edge features show the same variation with intensity in the range of temperatures for which the bipolaron signal can be measured.

A characteristic time  $\tau$  for the decay of photoexcited bipolarons can be estimated from the variation of the photoinduced absorption signal intensity as a function of the frequency at which the exciting laser is chopped. In the low-frequency limit ( $\omega\tau \ll 1$ ) the signal is roughly independent of frequency, while in the high-frequency limit ( $\omega\tau \gg 1$ ) it decreases with increasing frequency in a way that depends on the details of the recombination kinetics. The region of crossover ( $\omega\tau \sim 1$ ) provides the desired estimate of  $\tau$ . We show in Fig. 7 the variation of the photoinduced change in sample transmission at 1 eV as a function of chop frequency  $\omega$ , at a temperature of 80 K. The sample was photoexcited with the 488-nm line of the

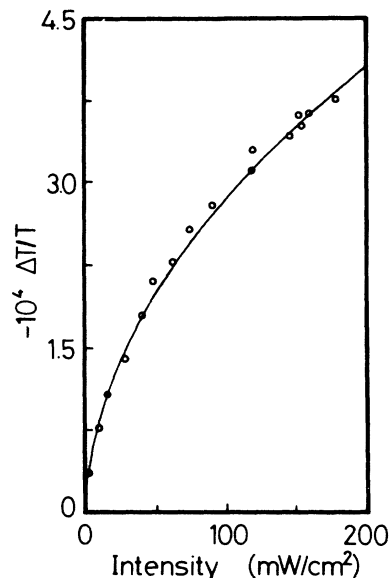


FIG. 6. The excitation intensity dependence of the photoinduced bipolaron absorption peak at 1 eV recorded at 80 K with excitation at 488 nm.

argon-ion laser. Below  $100 \text{ s}^{-1}$  the signal is nearly independent of frequency, above  $1000 \text{ s}^{-1}$  it decreases approximately as  $\omega^{-1/2}$ , with a crossover near  $300 \text{ s}^{-1}$ . Because the high-frequency behavior of the curve in Fig. 7 is, as expected from the intensity dependence, found to be inconsistent with a monomolecular decay (which would, instead, yield a high-frequency dependence of the form  $\omega^{-1}$ ), the crossover at  $300 \text{ s}^{-1}$  cannot be simply interpreted as an inverse excitation lifetime. We consider, rather, that the photoexcited bipolarons exhibit a range of lifetimes, and interpret the time  $\tau \sim 3 \text{ ms}$  indicated by the data in Fig. 7 as a characteristic time for the decay of the longest-lived excitations. We also note that at 80 K the frequency dependence of the transient absorption signal at 1.78 eV is identical to that shown in Fig. 7, again

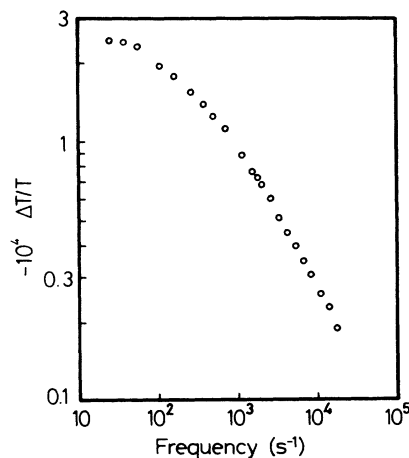


FIG. 7. The chop-frequency dependence of the photoinduced bipolaron absorption peak at 1 eV recorded at 80 K with excitation at 488 nm.

supporting its assignment to electric-field modulation of the band edge by the charged bipolarons.

In Fig. 8 we show the temperature dependence of the photoinduced absorption at 1 eV. The photoinduced bipolaron signal starts to decrease rapidly above 150 K and disappears above 200 K. A very similar behavior has been seen for the photoinduced absorption associated with charged solitons in *trans*-polyacetylene, and has been attributed there to a reduction in the excited-state lifetime due to an increase in mobility resulting in more frequent recombination events.<sup>24</sup> Comparable behavior is also seen for the photoinduced infrared modes in poly(thiophene) (Ref. 25) and for the bipolaron subgap transitions in PPV.<sup>5,14</sup>

For that range of probe photon energies where the absorption coefficient of the sample is large, interpretation of the photoinduced absorption data is complicated by effects due to sample heating. These effects are most noticeable at temperatures above 150 K, where a larger temperature dependence of the band edge enhances the sensitivity of the transient absorption measurements to laser heating. Below 100 K we find that the photoinduced band-edge features show a similar temperature dependence to that of Fig. 8, but as the temperature is increased further the signal decreases, and above 150 K a new signal of opposite sign is detected. The latter is associated with the thermal modulation of the band edge due to laser heating. This assignment was confirmed by measuring the photoinduced absorption spectrum at room temperature, where no bipolaron peaks were detected and the observed band-edge features matched those of Fig. 2.

#### IV. DISCUSSION

PTV is an excellent polymer for optical characterizations of the type undertaken here in that the interband absorption is readily accessible with ion laser sources, the films are of good optical quality, and there is evidence that the polymer is well-ordered with a well-defined band edge. The absorption spectra in Fig. 1, particularly the spectrum obtained at 15 K, show clear evidence for vib-

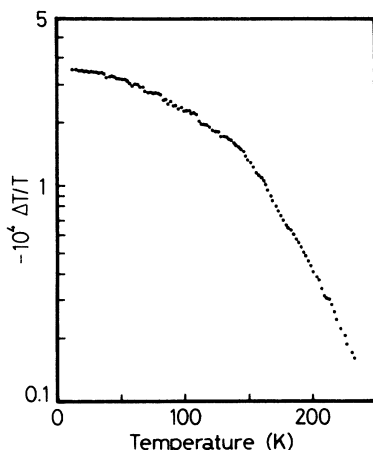


FIG. 8. The temperature dependence of the photoinduced bipolaron absorption peak at 1 eV with excitation at 488 nm.

ronic structure (peaks at 1.88, 2.07, and 2.25 eV), indicating that the ground-state and excited-state configurations are distinct (in the current idiom, the excited states are described as polarons). This vibronic structure is readily obscured if there is a distribution in electronic band gap, introduced through disorder in the polymer, and hence, although the observed resonance Raman dispersion indicates that such disorder is present, we conclude that it cannot be very great.

The resolution of the vibronic structure on the interband absorption indicates that the width of the interband absorption is due in large measure to the vibrational coupling to the electronic excited state. Peaks in the vibronic structure are seen at 1.88, 2.07, and 2.25 eV, with the maximum absorption at 2.25 eV. The relation between these peaks and the band gap as defined in the "rigid-band" sense ( $2\Delta$ ) is determined through the Frank-Condon factors, and we expect this to be close to the absorption maximum at 2.25 eV.

#### A. Bipolaron formation

PTV does not possess the degenerate ground state that is a characteristic of *trans*-polyacetylene.<sup>17</sup> The fundamental excitations of the chain are thus nontopological, polaron states (singly charged polaron, doubly charged bipolaron, or neutral polaron-exciton).<sup>16,25</sup> The energy difference between the two senses of bond alternation (aromatic and quinoid) forces the kink excitation characteristic of *trans*-polyacetylene to remain bound to its complementary antikink, and the resultant polaron state has associated with it two energy levels within the gap. The extent of the polaron state along a polymer chain is determined in one-electron models by the degree to which the ground-state degeneracy is lifted.<sup>17</sup> The case of near degeneracy allows the polaron states to be relatively extended with electronic levels near the center of the gap, while strong breaking of the degeneracy keeps them much more compact with levels near the band edges. Hence, the degree of nondegeneracy can be conveniently parametrized by an experimentally accessible ratio  $\omega_0/\Delta$ , where  $2\omega_0$  is the separation between the intragap polaron-state energy levels and  $2\Delta$  is the energy gap. The nondegeneracy can also be expressed more formally within the theoretical framework as a confinement parameter  $\gamma$ , which is related to the ratio  $\omega_0/\Delta$ .<sup>16</sup>

Electron-hole pairs produced by photoexcitation across the band gap may either remain bound to form the neutral, intrachain polaron exciton, or if they are able to separate, may form metastable charged excitations. These must initially be in the form of singly charged polarons, but though they may be present as a transient species, they do not appear to be detected under the experimental conditions used in the present work, for which excitations with lifetimes comparable to the chop frequencies used for the pump beam are detected. PTV is similar in this respect to PPV (Ref. 5) and to polythiophene.<sup>19</sup> The evidence that polarons are not the dominant long-lived charged excitation in these materials comprises (a) the presence, for all three polymers, of only two photoinduced optical-absorption bands, assigned to

transitions between the two gap states and the band edges for bipolarons (a third transition between the gap states is expected for polarons and should lie at an energy intermediate between the other two optical transitions), (b) the observation that these gap states lie too close to the band center to be consistent with the model of Fesser, Bishop, and Campbell,<sup>16</sup> in which  $\omega_0 \geq \Delta_0/\sqrt{2}$  for the singly charged polaron, and (c) the absence of photoinduced ESR associated with the charged photoexcitations for polythiophene.<sup>19</sup> Although the latter result has recently been challenged,<sup>26</sup> the close correspondence, for both polythiophene and PPV, between the observed photoinduced spectral features and those of dopant-induced charged excitations previously identified as bipolarons<sup>27</sup> [where there is agreement over the interpretation of ESR (Refs. 28 and 29)] strongly supports the proposed assignment. Light-induced ESR measurements remain to be undertaken for PTV but current indications are that the photoinduced absorption spectra are consistent with the photogeneration of long-lived bipolarons.

These bipolarons must be formed by the coalescence of two like-charged polarons, which in spite of the Coulomb repulsion between the charges, results in the formation of a more strongly self-trapped excitation. This scheme is analogous to that for the photogeneration of long-lived charged solitons in polyacetylene in which the solitons are present as like-charged pairs on the same chain.<sup>23</sup> In both cases we consider that the singly charged polaron initially photogenerated is much less prone to self-localization onto a chain, and that these polarons can travel freely in a three-dimensional way through the material. However, the doubly charged excitation, bipolaron or soliton-antisoliton pair, is strongly self-localized, to the extent that interchain transport is a thermally activated hopping process, with characteristic activation energies of order 0.3 eV for polyacetylene.<sup>30</sup> Thus, at low temperatures, bipolarons will recombine with those of opposite charge only very slowly.

### B. Bipolaron confinement

As discussed above, the degree of nondegeneracy of the polymer electronic structure can be parametrized by a confinement parameter  $\gamma$ , which is given for the specific case of a bipolaron, in terms of the ratio  $\omega_0/\Delta$ , by:<sup>16</sup>

$$\gamma = \frac{\frac{\omega_0}{\Delta} \sin^{-1} \left( \frac{\omega_0}{\Delta} \right)}{\left[ 1 - \left( \frac{\omega_0}{\Delta} \right)^2 \right]^{1/2}}. \quad (2)$$

In those conjugated polymers for which photoexcited charged states have been studied, several of which are listed in Table I,  $\omega_0/\Delta \leq 0.45$  and Eq. (2) reduces to  $\gamma \approx (\omega_0/\Delta)^2$  to within about 10%. For PTV, the onset of the optical-absorption edge is at 1.8 eV, and if we take this energy as the lower limit for  $2\Delta$ , with  $2\omega_0 = 0.56$  eV we find  $\omega_0/\Delta = 0.31$  and, from Eq. (2),  $\gamma = 0.10$ . This value is smaller than those in all the other nondegenerate ground-state materials studied to date. In particular, we note that replacement of the phenylene in PPV by a

thienylene in PTV significantly reduces the degree of confinement.

The approximately equal intensity of the two bipolaron optical transitions in Fig. 5 and their asymmetric displacement about midgap is inconsistent with the predictions of the noninteracting electron continuum model.<sup>16,31</sup> The same effects are seen for PPV (Ref. 5) and polythiophene<sup>19</sup> and have recently been considered theoretically by inclusion of on-site and intersite electron-electron interaction terms in the model Hamiltonian.<sup>32,33</sup> Weak on-site interactions are found not to greatly alter the predictions of the noninteracting model for the relative transition intensities and only when the strong-coupling limit is approached can the theories obtain intensity ratios consistent with experiment. Weak interactions can, however, explain the asymmetric displacement of the levels. Within a perturbation-theory treatment<sup>32</sup> the two bipolaron transitions are found at energies

$$E_{\pm} = \Delta \pm \omega_0 - U_{\text{eff}}, \quad (3)$$

where  $U_{\text{eff}} = aU_0/3l$ , with  $U_0$  the bare Coulomb repulsion for two electrons on one  $p_z$  orbital, and  $l/a$  the length in units of carbon-carbon bonds for the bipolaron. An estimate of the interaction strength  $U_{\text{eff}}$  can thus be obtained from the observed difference between the gap energy and the sum of the two bipolaron transition energies. We need an accurate value of  $2\Delta$  here. If we use the band-edge value of 1.8 eV for  $2\Delta$ , we find  $U_{\text{eff}} \approx 0.18$  eV, somewhat smaller than the values found for other polymers,<sup>5,19</sup> but a value of  $2\Delta$  taken at the peak of the optical absorption, at 2.25 eV gives  $U_{\text{eff}} \approx 0.4$  eV, which is more in line with values for other polymers.

In light of this discussion, it is necessary to consider what effect, if any, Coulomb interactions have upon the energy spacing  $2\omega_0$ , and hence the  $\gamma$  value derived from Eq. (2). We have previously shown for PPV (Ref. 5) that the value of  $2\omega_0$  is significantly smaller for charged-bipolaron than for neutral polaron-exciton states. This is again contrary to the expectations of one electron theory<sup>16</sup> for which  $2\omega_0$  is dependent only on the difference in occupancy of the upper and lower levels, i.e.,  $n_+ - n_-$ , such that polaron-exciton and bipolaron states,

TABLE I. Estimated confinement parameters for several conjugated polymers. In each case  $\gamma$  was determined from Eq. (2) using values for  $\omega_0$  from this work and previously published photoinduced absorption spectra (Refs. 5 and 19). We have taken  $2\Delta$  as the energy at the onsets of the respective  $\pi$ - $\pi^*$  absorptions; these values therefore underestimate  $2\Delta$  and overestimate  $\omega_0/\Delta$  and hence  $\gamma$ .

Material	$2\Delta$ (eV)	$\omega_0/\Delta$	$\gamma$
<i>trans</i> -polyacetylene	1.4	0	0
poly(2,5-thienylene vinylene)	1.8	0.31	0.10
polythiophene	2.2	0.36	0.14 <sup>a</sup>
poly( <i>p</i> -phenylene vinylene)	2.5	0.40	0.18 <sup>b</sup>

<sup>a</sup> The analysis of resonance Raman scattering data in Ref. 19 gives  $\gamma = 0.27$ .

<sup>b</sup> The  $\gamma = 0.27$  value quoted in Ref. 5 was incorrectly derived from the observed  $\omega_0/\Delta$  value.

both with  $n_+ = n_-$ , should have the same level spacing. We believe that electrostatic repulsion between the two charges present on a bipolaron provides energy to increase its extent along the polymer chain, resulting in a reduced level splitting. As a consequence, the values of  $\gamma$  listed in Table I are expected to somewhat underestimate the strength of the confinement arising purely from the energy difference between phases with reversed senses of bond alternation.

The data in Table I show a correlation between band gap  $2\Delta$  and the confinement parameter  $\gamma$ . In the simplest models<sup>16,31</sup> for nondegenerate ground-state conjugated polymers,  $\Delta$  is taken to be of the form  $\Delta = \Delta_i + \Delta_e$ , where  $\Delta_i$  is an intrinsic component sensitive to electron-phonon coupling and  $\Delta_e$  a constant extrinsic component. According to this ansatz, and following Ref. 16,  $\gamma$  is defined as

$$\gamma \equiv \frac{\Delta_e}{\lambda\Delta}, \quad (4)$$

where  $\lambda$  is the electron-lattice coupling constant. If we assume that  $\lambda$  is similar for all these polymers, then Eq. (4) implies that the increasing values of  $\gamma$  arise simply from the increasing relative strength,  $\Delta_e/\Delta$ , of the extrinsic component of the gap. The difficulty though, as we have pointed out previously,<sup>5</sup> is that the values of  $\gamma$  derived from the ratio of  $\omega_0/\Delta$  for the photoinduced bipolarons are much smaller than we would expect to get if we use reasonable estimates for the electron-phonon coupling strength and the intrinsic and extrinsic components of the gap in Eq. (4).

Finally, even though the question as to whether or not electron-electron interaction effects can, in general, simply be included as a perturbation to the results of noninteracting models remains somewhat open, the basic stability of polaronic excitations as the preferred charge carriers following photoexcitation is strongly confirmed by the results presented here. The importance of factors, such as disorder, in achieving this stabilization has yet, however, to be fully considered.

### C. Neutral excitations

In contrast to the relatively strong photoluminescence of PPV (quantum yield  $\sim 0.08$ ), PTV shows very little photoluminescence (quantum yield  $\sim 10^{-5}$ ). In addition, whereas the emission from PPV consists of a well-defined band with resolved vibrational structure and appears below the absorption edge, the weak emission in PTV is above the edge and has a spectral profile dependent upon excitation energy. This suggests that the emission from PTV may be due to hot geminate recombination rather than the decay of thermally equilibrated singlet excitons as in PPV. Furthermore, while a transient absorption feature identified as a triplet-triplet transition has been reported in PPV,<sup>14</sup> we have not seen any corresponding feature in PTV during photoexcitation. Hence, although both singlet and triplet excitons are seen to play an important role in the photophysics of PPV, they apparently do not in that of PTV. These excitonic effects are rather more characteristic of a molecular semiconductor-like an-

thracene<sup>34</sup> than a conventional (i.e., inorganic) semiconductor and it is of obvious fundamental interest to identify the factors that determine the importance of this molecular contribution to the overall semiconductive response of conjugated polymers. We discuss some of these below.

Measurements of the excitation-polarization dependence of the photogeneration of bipolarons in PPV indicate that, as is also the case for solitons in *trans*-polyacetylene, the separation of electron-hole pairs onto neighboring chains inhibits geminate recombination, facilitating the formation of isolated charge carriers.<sup>5</sup> The strength of interchain coupling should also influence the stability of excitonic states, not only through its effect on charge separation but also, and probably more importantly, by its enhancement or limitation of exciton motion to recombination centers.<sup>5</sup> This coupling depends on the extent of  $\pi$ -electron overlap between carbon atoms on neighboring chains, as well as hybridization through the pendant hydrogens.<sup>35</sup> The presence in PTV of sulfur heteroatoms, which may enhance the interchain interactions is a further complication. A complete assessment of the importance of interchain coupling will require a detailed comparison of structural data for PPV and PTV.

Considering the properties of an isolated chain in the one-electron limit, the intrinsic stability of charged and neutral electronic excitations in conjugated polymers is probably also correlated, through its dependence on  $\pi$ -electron delocalization, with the band gap. The heterogeneous electronic wave functions that result from poor overlap of the wave functions of molecular subunits along a polymer chain, such as the phenylene and vinylene moieties in PPV, result in reduced bandwidths and larger band gaps more characteristic of molecular crystals. This wave-function heterogeneity should, as is the case in the extreme of the subunits of true molecular crystals,<sup>34</sup> favor the formation of excitons. Similarly, it would tend to inhibit the formation of extended excited electronic states, and is therefore consistent with the difference in the degree of confinement of bipolarons in PPV and PTV.

Even where generation of excitonic states is significant, their contribution to the measured properties following photoexcitation depends greatly on the possible decay channels linking the excited and ground states. When nonradiative decay is important, the luminescence expected for the radiative recombination of singlet excitons can become very weak and short lived. Included among the typical nonradiative recombination mechanisms in such materials is exciton-exciton collisional annihilation, a process that strongly depends upon the length of the conjugated sequence.<sup>5</sup> The latter is invoked to explain the order of magnitude decrease in quantum yield and decay time seen in going from the effective PPV oligomer bispropyl(*trans,trans*-1,4-distyrylbenzene) to the PPV polymer.<sup>5</sup> Disorder can thus influence the recombination of excitons by its limitation of the degree of conjugation as for instance appears to be the case in polydiacetylenes.<sup>36</sup> The presence of photogenerated or dark charge carriers is also important, as it causes a reduction in the luminescence yield.<sup>37</sup> In addition, nonradiative decay involving multiple-phonon emission should show a strong depen-



dence upon electron-phonon coupling and band gap.<sup>38</sup> Hence, a clarification of the relative roles of different materials parameters in influencing the nature of the dominant photoexcited states is an involved problem requiring considerable further study.

*Note added in proof.* Y. Furukawa, A. Sakamoto, and M. Tasumi [J. Phys. Chem. **93**, 5354 (1989)] have recently reported a similar dispersion effect in the resonance Raman spectra of PTV.

## ACKNOWLEDGMENTS

Research at the Cavendish Laboratory is supported by the United Kingdom Science and Engineering Research Council, and by British Petroleum, p.l.c. One of us (D.D.C.B.) thanks Unilever, p.l.c. and Corpus Christi College, University of Cambridge for the provision of partial support.

- <sup>1</sup>See for example, *Nonlinear Optical Properties of Organic Molecules and Crystals*, edited by D. S. Chemla and J. Zyss (Academic, London, 1987); *Nonlinear Optical Effects in Organic Polymers*, NATO Advanced Study Institute, Series E162 (Kluwer, Dordrecht, 1989); *Nonlinear Optical and Electroactive Polymers*, edited by P. N. Prasad and D. R. Ulrich (Plenum, New York, 1988); *Nonlinear Optical Properties of Polymers*, Vol. 109 of the *Proceedings of the Materials Research Society Symposium*, edited by A. J. Heeger, J. Orenstein, and D. R. Ulrich (MRS, Pittsburgh, 1988).
- <sup>2</sup>T. Kaino, K.-I. Kubodera, S. Tomaru, T. Kurihara, S. Saito, T. Tsutsui, and S. Tokito, *Electron. Lett.* **23**, 1095 (1987); B. P. Singh, P. N. Prasad, and F. E. Karasz, *Polymer* **29**, 1940 (1988); D. McBranch, M. Sinclair, A. J. Heeger, A. O. Patil, S. Shi, S. Askari, and F. Wudl, *Synth. Met.* **29**, E85 (1989); D. D. C. Bradley and Y. Mori, *Jpn. J. Appl. Phys. Pt. I* **28**, 174 (1989); D. D. C. Bradley, *Makromol. Chem.; Macromol. Symp.* (to be published); C. Bubeck, A. Kaltbeitzel, and D. Neher, *Springer Series in Solid-State Sciences* (Springer, New York, 1989), Vol. 91, p. 214.
- <sup>3</sup>T. Kaino, K.-I. Kubodera, H. Kobayashi, T. Kurihara, S. Saito, T. Tsutsui, S. Tokito, and H. Murata, *Appl. Phys. Lett.* **53**, 2002 (1988).
- <sup>4</sup>D. D. C. Bradley, *J. Phys. D* **20**, 1389 (1987); and references therein.
- <sup>5</sup>R. H. Friend, D. D. C. Bradley, and P. D. Townsend, *J. Phys. D* **20**, 1367 (1987); and references therein.
- <sup>6</sup>S. Yamada, S. Tokito, T. Tsutsui, and S. Saito, *J. Chem. Soc. Chem. Commun.* **1987**, 1448; S. Tokito, T. Momii, H. Murata, T. Tsutsui, and S. Saito, *Polymer* (to be published); H. Murata, S. Tokito, T. Tsutsui, and S. Saito (unpublished).
- <sup>7</sup>Y. Furukawa, M. Akimoto, and I. Harada, *Synth. Met.* **18**, 151 (1987).
- <sup>8</sup>S. Lefrant, E. Perrin, J. P. Buisson, H. Eckhardt, and C. C. Han, *Synth. Met.* **29**, E91 (1989); D. D. C. Bradley, Ph.D. thesis, University of Cambridge, 1987.
- <sup>9</sup>H. Kuzmany, *Phys. Status Solidi B* **97**, 521 (1980); D. B. Fitch, *Mol. Cryst. Liq. Cryst.* **83**, 95 (1982).
- <sup>10</sup>B. Horowitz, *Solid State Commun.* **41**, 729 (1981); E. Ehrenfreund, Z. Vardeny, O. Brafman, and B. Horowitz, *Phys. Rev. B* **36**, 1535 (1987); G. Zerbi, C. Castiglioni, J. T. Lopez-Navarrete, T. Bogang, and M. Gussoni, *Synth. Met.* **28**, D359 (1989).
- <sup>11</sup>Z. Vardeny, E. Ehrenfreund, O. Brafman, A. J. Heeger, and F. Wudl, *Synth. Met.* **18**, 183 (1987).
- <sup>12</sup>R. A. Lawrence (private communication).
- <sup>13</sup>We are currently undertaking such an analysis for PTV and the results will be published elsewhere.
- <sup>14</sup>D. D. C. Bradley, N. F. Colaneri, and R. H. Friend, *Synth. Met.* **29**, E121 (1989).
- <sup>15</sup>L. S. Lichtmann, A. Sarhangi, and D. B. Fitch, *Solid State Commun.* **36**, 869 (1980); W. Hayes, C. N. Ironside, J. F. Ryan, R. P. Steele, and R. A. Taylor, *J. Phys. C* **16**, L729 (1983).
- <sup>16</sup>K. Fesser, A. R. Bishop, and D. K. Campbell, *Phys. Rev. B* **27**, 4804 (1983).
- <sup>17</sup>A. J. Heeger, S. Kivelson, J. R. Schrieffer, and W.-P. Su, *Rev. Mod. Phys.* **60**, 781 (1988).
- <sup>18</sup>C. M. Foster, Y. H. Kim, N. Uotani, and A. J. Heeger, *Synth. Met.* **29**, E135 (1989).
- <sup>19</sup>Z. Vardeny, E. Ehrenfreund, O. Brafman, M. Nowak, H. Schaffer, A. J. Heeger, and F. Wudl, *Phys. Rev. Lett.* **56**, 671 (1986).
- <sup>20</sup>Y. H. Kim, D. Spiegel, S. Hotta, and A. J. Heeger, *Phys. Rev. B* **38**, 5490 (1988).
- <sup>21</sup>F. L. Pratt, K. S. Wong, W. Hayes, and D. Bloor, *J. Phys. D* **20**, 1361 (1987).
- <sup>22</sup>J. Orenstein, G. L. Baker, and Z. Vardeny, *J. Phys. (Paris) Colloq.* **44**, C3-407 (1983).
- <sup>23</sup>N. F. Colaneri, R. H. Friend, H. E. Schaffer, and A. J. Heeger, *Phys. Rev. B* **38**, 3960 (1988).
- <sup>24</sup>Z. Vardeny, J. Orenstein, and G. L. Baker, *Phys. Rev. Lett.* **50**, 2032 (1983).
- <sup>25</sup>H. Schaffer and A. J. Heeger, *Solid State Commun.* **59**, 415 (1986).
- <sup>26</sup>K. Kaneto, F. Uesugi, and K. Yoshino, *J. Phys. Soc. Jpn.* **57**, 1859 (1988).
- <sup>27</sup>D. D. C. Bradley, G. P. Evans, and R. H. Friend, *Synth. Met.* **17**, 651 (1987).
- <sup>28</sup>K. Yoshino, T. Takiguchi, S. Hayashi, D. H. Park, and R. Sugimoto, *Jpn. J. Appl. Phys. Pt. 1* **25**, 881 (1986).
- <sup>29</sup>A. Pron, F. Genoud, M. Nechtschein, and A. Rousseau, *Synth. Met.* **31**, 147 (1989).
- <sup>30</sup>P. D. Townsend and R. H. Friend, *Phys. Rev. B* **40**, 3112 (1989).
- <sup>31</sup>S. A. Brazovskii and n. n. Kirova, *Pis'ma Zh. Eksp. Teor. Fiz.* **33**, 6 (1981) [*JETP Lett.* **33**, 4 (1981)].
- <sup>32</sup>D. K. Campbell, D. Baeriswyl, and S. Mazumdar, *Synth. Met.* **17**, 197 (1987).
- <sup>33</sup>U. Sum, K. Fesser, and U. Buttner, *Solid State Commun.* **61**, 607 (1987).
- <sup>34</sup>M. Pope and C. E. Swenberg, *Electronic Processes in Organic Crystals* (Oxford University Press, New York, 1982).
- <sup>35</sup>P. Vogl and D. K. Campbell, *Phys. Rev. Lett.* **62**, 2012 (1989).
- <sup>36</sup>T. Hattori, W. Hayes, and D. Bloor, *J. Phys. C* **17**, L881 (1984).
- <sup>37</sup>D. D. C. Bradley and R. H. Friend, *J. Phys. Cond. Matter* **1**, 3671 (1989); H. B. Gu, T. Takiguchi, S. Hayashi, K. Kaneto, and K. Yoshino, *J. Phys. Soc. Jpn.* **56**, 3997 (1987).
- <sup>38</sup>P. L. Danielsen, R. C. Ball, *J. Phys. (Paris)* **46**, 1611 (1985).